ISSN: 2320 - 4230

Journal of Drug Discovery and Therapeutics

Available Online at www.jddt.in

CODEN: - JDDTBP (Source: - American Chemical Society)

Volume 11, Issue 2, March-April: 2023, 56-70

Research Article

Design of Formulation, Optimization and Evaluation of Nanosponges of Selected Drug by Using QBD Technology

***Popin Kumar[1], Dr Shailesh M Kewatkar[2]**

[1]Research Scholar, Sunrise University Campus, Bagar Rajput, Alwar, Rajasthan 301028
[2]Professor, Department of Pharmacy, Rajarshi Shahu College of Pharmacy, Buldhana, Maharashtra, India

Article Info: Received: 26-01-2023 / Revised: 06-02-2023 / Accepted: 27-02-2023
DOI: https://doi.org/10.32553/jddt.v11i2.464
Corresponding author: Popin Kumar (popinkumar4761@gmail.com)
Conflict of interest: No conflict of interest.

Abstract:

When one chemical material (the solute) can dissolve in another chemical substance (the solvent) of the same sort, the resulting is homogeneous solution. Whether or not a chemical is soluble depends on a number of factors, including pressure, temperature, and the nature of the solvent being utilized. How soluble something is in a given solvent may be measured at its saturation concentration, when further addition of the solute no longer increases the concentration of the solute in the solution (Lachman L et al., 1986). The solvent is often a liquid comprising one or more substances. It is more common to vocalize a solid solution than a gaseous one.

Introduction

The solvent is often a liquid comprising one or more substances. It is more common to vocalize a solid solution than a gaseous one. It's possible to find compounds that are completely miscible (infinitely soluble) in water, like ethanol, and others that are completely insoluble, like silver chloride. Subtly soluble compounds are typically referred to as "insoluble" (Clugston M et al., 2000). Solubility is the outcome of dissolution and phase joining processes interacting in opposition under circumstances of dynamic equilibrium (e.g., precipitation of solids). Solubility is the steady state that results when the two processes proceed at equal rates. When the equilibrium solubility is exceeded, supersaturated solutions may occur; these solutions are metastable (Myrdal P et al., 2000).

Material engineering of the actives (supercritical fluid technology, micellar solubilization; particle size reduction; hybridization; crystal engineering etc.), as shown in Fig. 1, and formulation approaches (Kumar A et al., 2011) are two ways to alter the API's dissolution or solubility (microemulsion; complexation by cyclodextrins; solid dispersions, cosolvent approach; addition of polymers; hydrotrophy; pH adjustment; prodrug approach etc). Class II actives (those with poor solubility and high permeability) and

class IV actives (those with poor solubility and low permeability) are good candidates for improving solubility and, therefore, oral bioavailability.

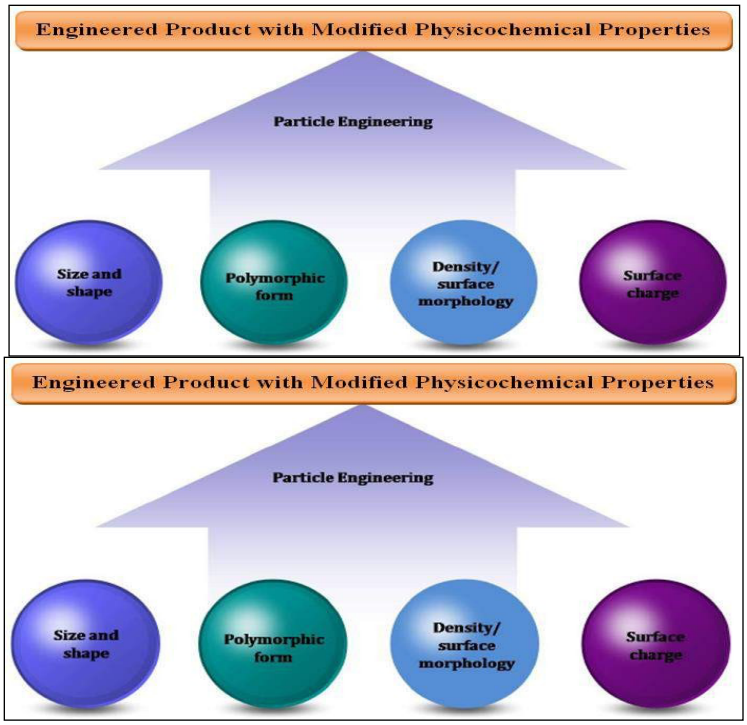

Figure 1: Drug Particle Engineering: Concept

There are several advantages of using nanomaterials as drug carriers. In order to improve therapeutic efficacy, nanocarriers can do the following: I increase aqueous solubility and protect drugs dissolved in the systemic circulation, thereby improving their pharmacokinetic and pharmacological traits; ii) target the liberation of actives in a tissue- or cell-specific manner, thereby preventing The actives' accumulation in the liver, kidneys, spleen, and other non-targeted organs; and iii (Burgess P et al., 2010 and Farokhzad O et al., 2009). Figs. 1.3 and 1.4 shows that the advantages and disadvantages of various nanovectors for various therapeutic applications, as well as the molecular targets to which they are relevant, are becoming more clear.

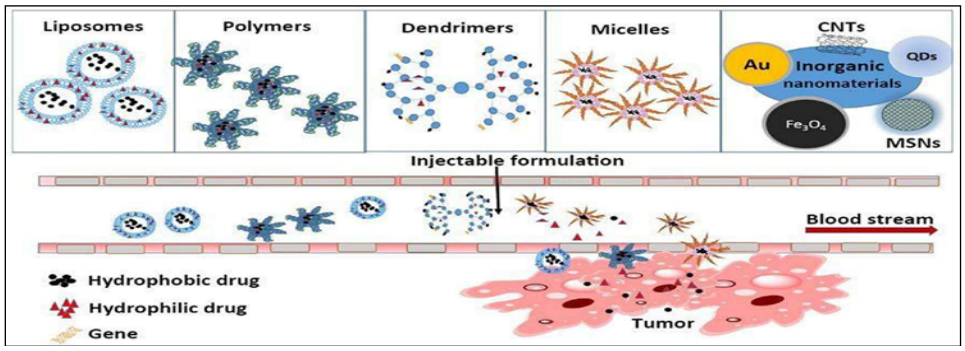

Figure 2: Nanomaterials used as drug carriers in different therapy of diseases

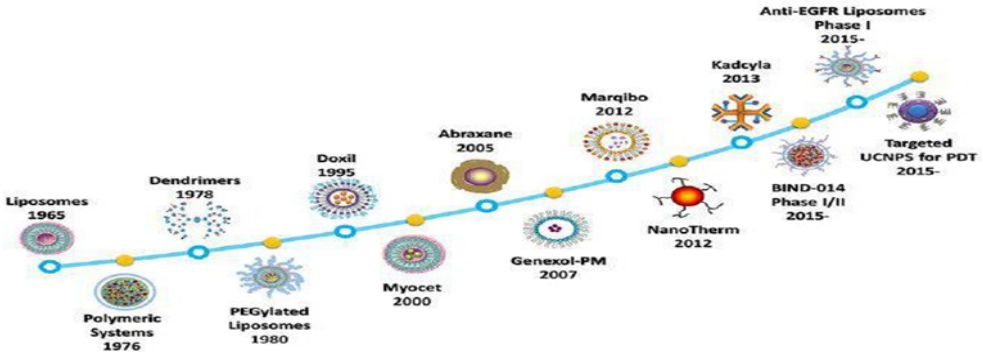

Figure 3: Timeline of the development of nanomedicines

A Carrier Role for Nanosponges

Nanosponge technology has advanced the state of the art in excipients, leading to claims of fewer adverse effects, more stability, more refined aesthetics, and more nimble formulations. Toxic, mutagenic, allergic, or irritant properties are absent from sponges. Nanosponges are very small structures that resemble mesh (Bolmal et al., 2013). Sponge NPs have several advantages to supplemental NPs, such being insoluble in water and organic solvents, being porous, being non-toxic, and being stable at temperatures up to 300oC. While nanosponges were first developed as a topical medication delivery device, they have now been shown to be safe and effective when administered orally and intravenously (Yadav et al., 2013).

Hypercrosslinked cyclodextrin is positioned in a three-dimensional network to form nanosponges. Spongy NPs formed by nanosponges have a size of less than 500 nm, making them easily able to circulate throughout the body. Toxins, fragments, and secretions produced by cancer cells themselves may be absorbed by these'sponges (Hu C et al., 2013, Hu C et al., 2011 and Hu C et al., 2013). They are able to enclose a wide variety of molecules, ions, gases, and macromolecules because to their spherical shape and negative surface charge. Thus, NSGs aim to improve the efficacy of chemotherapies by eliminating drug-resistant cells (Hu C et al., 2013, Hu C et al., 2015 and Trotta F et al., 2014). There are more than 3,000 nanosponges in the erythrocyte membrane that may be used as a disguise. After nanosponges are completely saturated with toxins, the liver may dispose of them in a non-lethal manner. Because of this, they are adaptable to every kind of cancer or poisoning characterized by dysregulation or anomalies in cellular membranes.

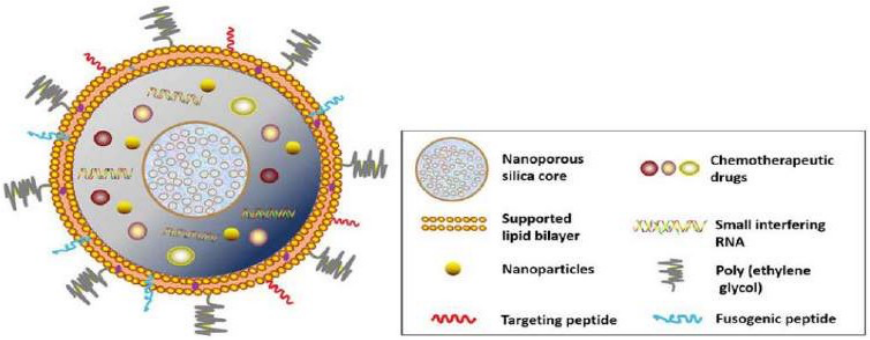

Figure 4: Lipid bilayer-wrapped nanoporous drug delivery system in protocells. It can be decorated with multi-types chemotherapy agents and surface targeting molecules

Aim & Objective

The purpose of this research was to use an appropriate factorial design to create, construct, and analyze Rasagiline mesylate-loaded nanosponges (NSGs).

These observations informed the driving forces for the current effort.

✓ To improve the solubility, encapsulation, dissolution rate, and oral therapeutic efficacy of rasagiline mesylate, the primary goal of the current invention was to construct a nanoporous drug delivery system.

✓ To investigate its potential use in enhancing bioavailability, sustained release/controlled release formulations, and overall stability.

Method of Nanosponges Formulation (NSGs): Nanosponges prepared from hypercross-linked β- cyclodextrins

Synthesis of β-CD Nanosponges:

Anhydrous -cyclodextrin (15.34 mmol) was dissolved in 100 mL of anhydrous dimethylformamide (DMF) by adding 17.42 g of the compound to a round bottom flask. The solution was then heated to 1000 degrees Celsius for 4 hours while 9.96 grams of dimethyl carbonate (carbonyldiimidazole) (61.42 mmol) were added. The clear block of hyper-cross-linked cyclodextrin was coarsely pulverized and an excess of deionized water was added after the condensation polymerization was finished to get rid of the DMF. Finally, Soxhlet extraction with ethanol was used to get rid of any lingering byproducts or unreacted chemicals. After drying the resulting white powder in a 60°C oven overnight, it was pulverized in a mortar. The resulting powder was then mixed with water. The lyophilized powder is made from the recovered colloidal fraction that remains suspended in water. Recovered nanosponges are spherical and measure on the order of a few microns in diameter. This is because the molar ratio of cyclodextrin to cross-linker is very flexible (i.e. 1:2, 1:4, 1:8). For preparing nanosponges, the molar ratio between the cross-linker and the nanosponges is 1:4. (Bagade O et. al., 2020).

Preparation of Drug-Loaded NS

Both 1:5 (Drug, BNS w/w) and 1:10 (Drug, BNS w/w) (Drug, NS w/w) (Drug NS 1:2 and 1:4) complexes were developed. A magnetic stirrer was used to keep precisely measured amounts of NS 1:2, 1:4, and 1:8 suspended in 20 mL of distilled water for 24 hours before the estimated quantity of Drug was added, after which the mixture was sonicated for 10 minutes and left to swirl for another 24 hours. The uncomplexed medication was extracted as a residue below the colloidal supernatant after centrifugation at 2,000 rpm for 10 minutes. At a temperature of 20°C and a pressure of 13.33 mbar, the supernatant was lyophilized. A desiccator was used to keep the powder dry. For all preparations, a lot size of 1.0 g was set aside (Bagade O et. al., 2020).

Table 1: Design matrix of formulation

Step I: Synthesis of β-CD Nanosponges			
Ingredients	**F1**	**F2**	**F3**
DMF	100	100	100
β-CD:DMC (mmol or gm)	1:2	1:4	1:8
β-CD (gm)	17.42	17.42	17.42
β-CD (mmol)	15.34	15.34	15.34

DMC (gm)	19.92	39.84	79.68
DMC (mmol)	30.68	61.36	122.72
Ethanol (ml)	100	100	100
Dist. water (ml)	100	100	100
Step II: Preparation of RM-Loaded NS			
RM: β-CD (w/w)	1:5	1:10	1:15
β-CD NSGs	200	400	600
Dist. water (ml)	20	20	20
Centrifugation (RPM)	2000	2000	2000

Preparation of Drug-Loaded NS:

Drug-NS complexes with various weight ratios of 1:1, 1:2, 1:3, 1:4, and 1:5 (Drug, BNS w/w) were developed. Weighed amounts of NS (1:1, 1:2, 1:3, 1:4, and 1:5) were suspended in 20 mL of distilled water using a magnetic stirrer; the determined quantity of Drug was then added; the mixture was sonicated for 10 minutes and kept understirring for 24 hours. There were suspensions, and the uncomplexed medication was separated as a residue below the colloidal supernatant after centrifugation at 2,000 rpm for 10 minutes. At a temperature of 20°C and a pressure of 13.33 mbar, the supernatant was lyophilized. A desiccator was used to keep the powder dry. For all preparations, a 1.0 g lot size was set aside (Bagade O et. al., 2020).

Table 2: Design matrix of formulation

Step I: Synthesis of β-CD Nanosponges					
Ingredients	**F1**	**F2**	**F3**	**F4**	**F5**
β-CD:DMC (mmol or gm)	1:1	1:2	1:3	1:4	1:5
β-CD (gm)	17.42	17.42	17.42	17.42	17.42
β-CD (mmol)	15.34	15.34	15.34	15.34	15.34
DMC (gm)	9.96	19.92	29.88	39.84	49.8
DMC (mmol)	61.42	122.84	184.26	245.68	307.1
Ethanol (ml)	100	100	100	100	100
Step II: Preparation of RM-Loaded NS					
RM: β-CD (w/w)	1:1	1:2	1:3	1:4	1:5
β-CD NSGs	40	80	120	160	200
Dist. water (ml)	20	20	20	20	20
Centrifugation (RPM)	2000	2000	2000	2000	2000

Table 3: Monographic evaluation of Rasagiline mesylate

Test	**Specifications**	**Observations**
Appearance	White to almost white crystalline powder	White to almost white crystalline powder

Identification		
Solubility	Freely soluble in water and in Ethanol	Freely soluble in water and in Ethanol
Residual solvents	Meets the requirements	Complies
Melting point	150-152ºC	156-159ºC
Assay (% w/w)	98.0-102.0%	99.5%
UV spectrum	Absorption maximum at 265 Nm	Absorption maximum at 265 Nm
IR spectrum	The IR spectrum of the sample is concordant with the IR spectrum of RM crystalline USP reference/working standard.	The IR spectrum of RM have absorption peaks at (cm^{-1}) 3179.08**,** 3225.36,3278.39, 2992.98, 2871.49, 2804.01, 2594.75, 2353.69, 1925.57, 1743.33, 1626.66 etc
Loss on drying (% w/w)	NMT 0.5% w/w	0.4 % w/w
Residue on ignition (% w/w)	NMT 0.1% w/w	Nil

UV Spectroscopy:

Absorbance spectrum of a 15 µg/mL solution of RM in methanol was obtained from 400-200nm. As seen in the Fig, λ max was found to be at 265 nm and the absorbance was 0.237.

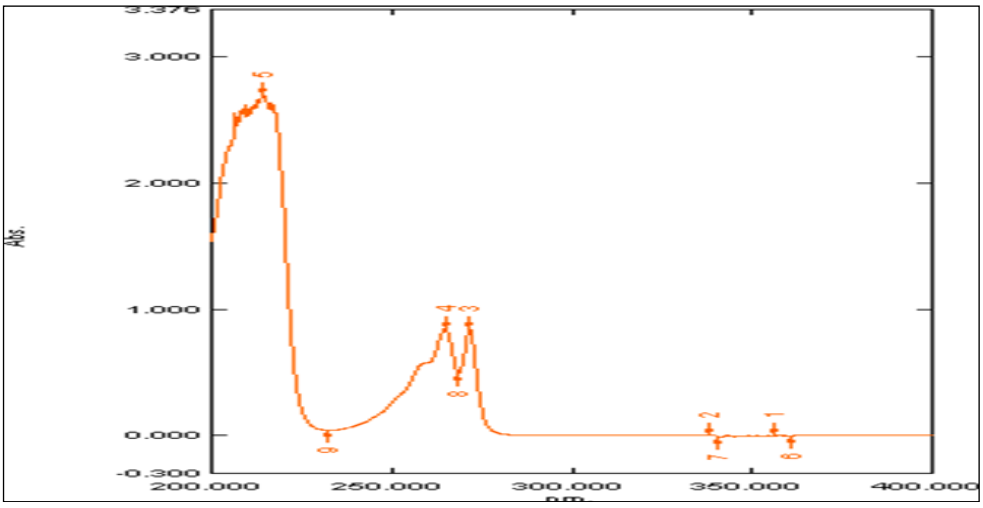

Figure 5: UV-visible spectrum of Rasagiline mesylate

Field Emission Scanning Electron Microscopy (FESEM):

Analysis of pure RM drug samples using FESEM revealed irregularly shaped particles with a mean diameter of roughly 5 m. This was detected at a higher resolution scale of 10000X.

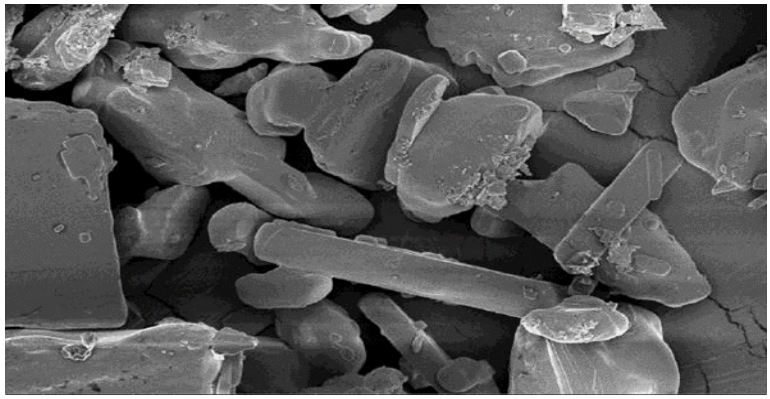

Figure 6: FESEM micrograph of rasagiline mesylate

Fourier Transform Infrared (FTIR) spectroscopy:

The peaks in the FTIR spectra of RM are quite comparable to the stated frequencies.

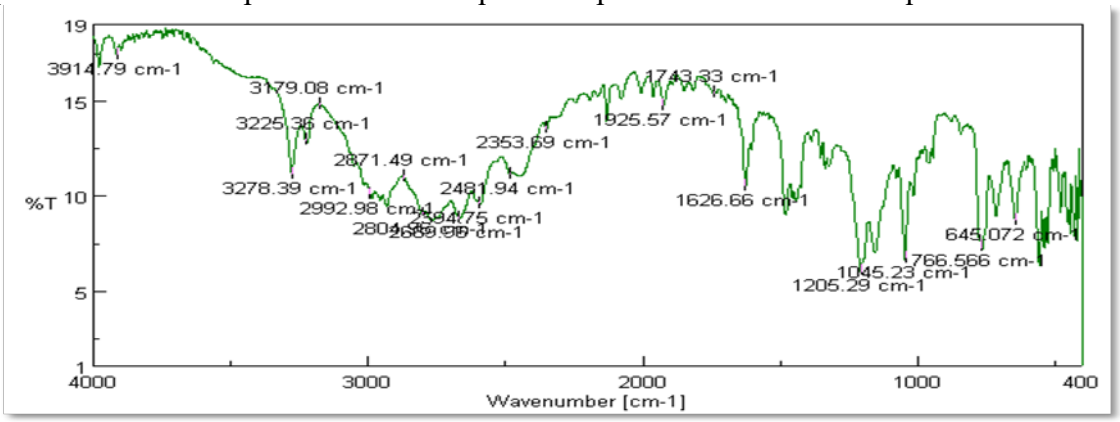

Figure 7: FTIR spectra of Rasagiline mesylate

Table 4: FTIR spectra observed frequencies of RM

Functionalgroups	**Reported frequency(cm^{-1})**	**Observed Frequency (cm^{-1})**
C=O stretching	1750-1735	1743.33
C=C=C stretching	2000-1900	1925.57
O=C=O stretching strong	2349	2353.69
O-H stretching	3300-2500	2481.94
S-H stretching	2600-2550	2594.75
O-H stretching weak, broad	3200-2700	2669.90
N-H stretching strong, broad	3000-2800	2804.12
C-H stretching alkane	3000-2840	2871.49
N-H stretching	3000-2800	2992.98
C-H stretching strong, sharp	3333-3267	3278.39
O-H stretching alcohol	3550-3200	3225.36
C-H stretching medium	3100-3000	3179.08
water OH Stretch	>3700	3914.79

Characterization (F6 Batch β-CD):

Surface morphology: This example of a FESEM picture shows (Fig 6.41). Rough agglomerates with a minute cavity of irregular form were seen on the surface, as seen by FESEM.

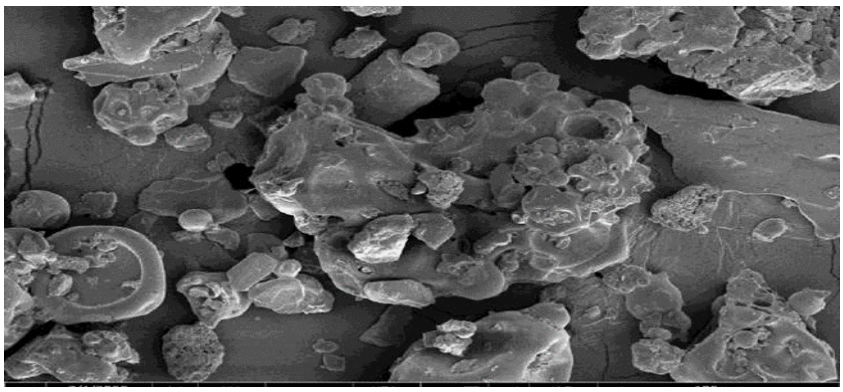

Figure 8: FESEM image of F6 Batch (with β-CD)

PXRD: PXRD diffractogram of RM-NSGs is depicted in Fig 6. 42. The diffractogram associated with the formulation (F6) exhibited series of sharp intense peaks and two major characteristic peaks was found at 2θ values 19.93, 20.03, 20.13 and 23.73, 23.83, 24.13, 24.23º. Thus, from the observation it was concluded that the formulation was found to be crystalline in nature.

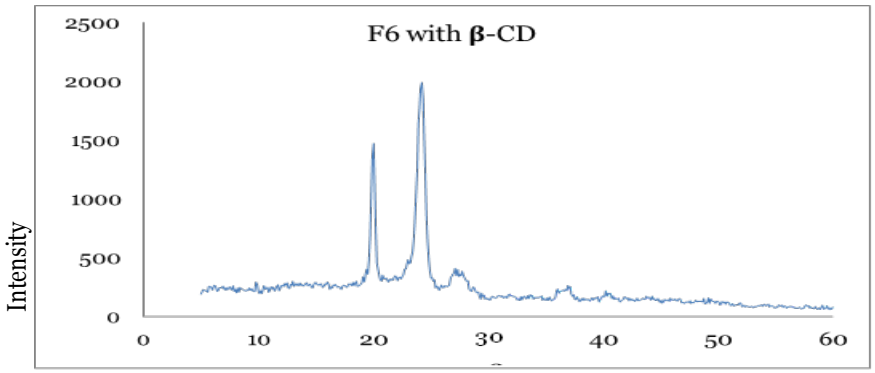

Figure 9: Powder X-ray diffraction pattern

Observation F6 Batch (with β-CD):

It was determined that the surface was made up of rough agglomerates with minute cavities that were uneven in form, as shown in a FESEM picture. PXRD analysis, on the other hand, showed that the formulation was crystalline. This meant that the option to scale using this way was also removed.

Characterization (F9 Batch with EC):

Particle size analysis by motic microscopy:

Particle size by motic microscopy was found to be 7.4 µm and maximum object perimeter was found to be 33.5 µm.

Table 5: Motic microscopy

The number of Objects :	11
Total Area :	**54.1 Squm**
Percentage of total area in the whole image :	0.472 %
Minimum object area :	0.13Squm
Maximum object area :	32.1Squm
Average object area :	Squm
Minimum object perimeter :	0.9µm
Maximum object perimeter :	33.5µm
Average object perimeter :	7.4µm

Figure 10: Motic microscopic image

Particle size and polydispersity index (PDI): As shown in Fig. 6. 44, the average particle size was 505 nm, with a PDI of 1.5.

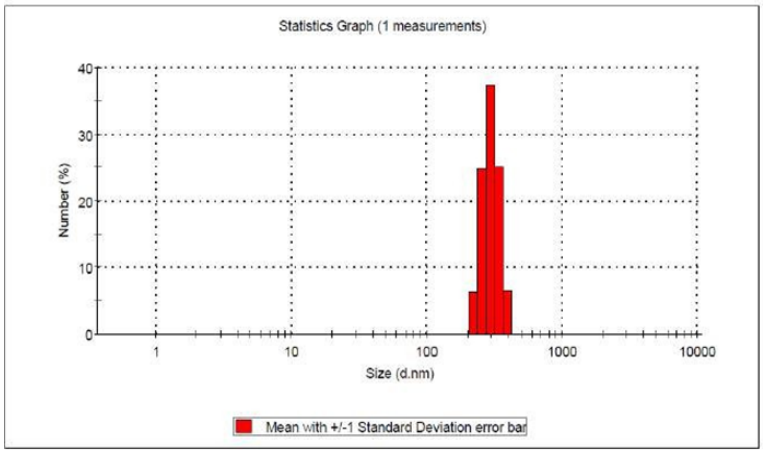

Figure 11: Particle size analysis

Surface morphology: Fig. 6.45 shows a FESEM picture. The FESEM scan showed the surface to be porous and somewhat spherical in form.

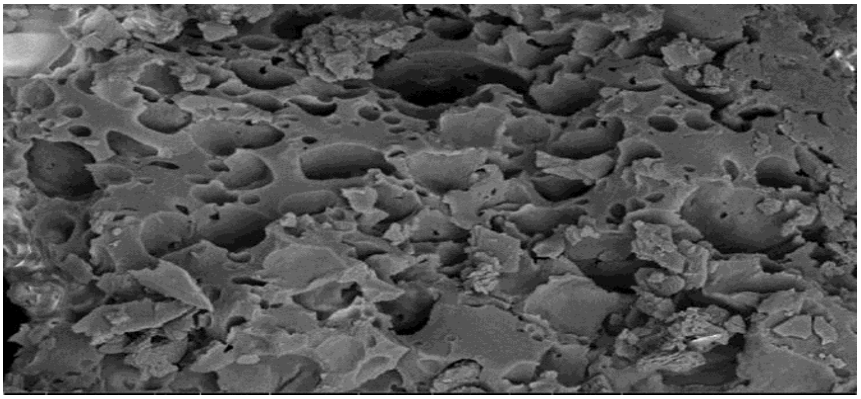

Figure 12: FESEM image with EC

Observation (F9 Batch with EC):

The finding led to the conclusion that the particle size was on the order of the nanometer. There was also a noticeable increase in the polydispersity index. The resultant particle was also porous and roughly spherical, as shown in the FESEM picture. As a result, this strategy was seen to be viable for future expansion. In light of this finding, we continued our work on formulation development and made many batches using varying proportions of polymer (EC): cross-linker (DMC), solvent such DMSO, and WPI as a stabilizer.

***In Vitro* Release Study:**

The in vitro release profile of RM, Marketed tablet, lyophilized RM-NSGs in phosphate buffer pH 7.4 at 37°C shown in Fig 6. 74-75. % drug release was not identical for all the batches. Initially the NSGs showed immediate release of RM, this may be due to release of drug from the surface of NSGs, followed by slow and controlled release of drug which was encapsulated in nanosponges. It was evident that, marketed tablet showed significant improvement in dissolution rate with respect to RM alone. Furthermore, the lyophilized RM-NSGs (F4) exhibit faster dissolution as compared to marketed formulation as well as plain RM and it was found to be 91.21%, 59.03 % and 33.43% respectively. The concentration of polymer and cross-linker affects the release rate of RM from nanoparticles. Conversely, as the polymer concentration increases, decrease in the rate and extent of drug release was observed. This may be due to increase in the density of the polymer matrix and also an increase in the diffusion path length that the drug molecules have to travel.

The calculated f1 (difference factor) value was equal to 65 and f2 (similarity factor) value was equal to 18 ensure different or non-equivalence of the two curves). Hence, the marketed tablet and the optimized formulation change dissolution profiles for nanosponges were dissimilar as f2 was 18.

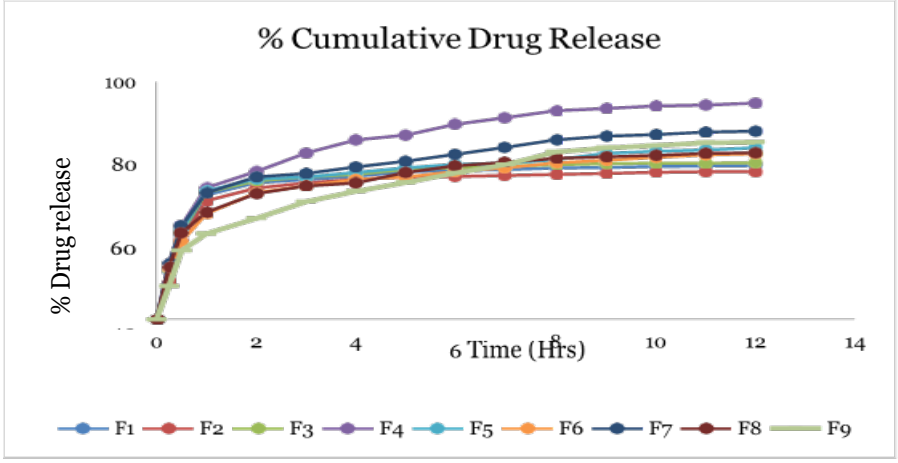

Fig 13: Release profile of different formulations of RM-NSGs

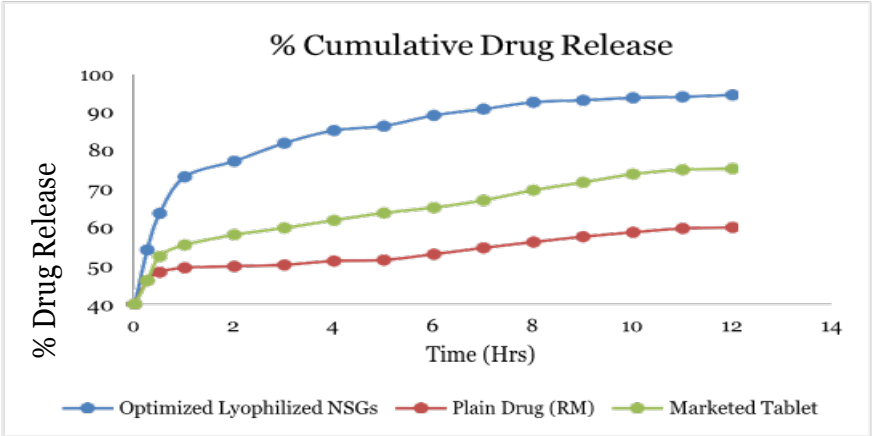

Figure 14: Release profile of Plain drug-RM, Marketed tablet and optimized lyophilized RM-NSGs

Stability study:

The stability study was implemented for optimized freeze dried RM-NSGs as per 6H guidelines, shown Table 6.32. Periodically samples were removed and checked for 1) physical appearance, entrapment efficiency, particle size and *in-vitro* drug release 2) solid state characterization. RM-NSGs filled capsule does not showed any significant change in above parameters indicating stability of RM-NSGs for a period of 6 months.

Table 6: 1) Stability study of RM-NSGs

Time (Month/s)	**Physical Appearance**	**Particle size (nm)**	**Entrapment Efficiency (%)**	**% CDR**	**Solubility (µg/ml)**
25±2°C/65± 5% RH					
0	white crystalline powder	108.38±0.25	92.49±1.76	90.77	145.74±0.887
3	white crystalline powder	109.86±0.11	92.20±1.83	90.98	142.85±2.713

6	white crystalline powder	110.01±0.10	92.20±1.83	89.93	141.38±1.296
30±2ºC/70±5% RH					
0	white crystalline powder	108.70±0.27	92.78±1.34	91.19	144.34±0.294
3	white crystalline powder	109.92±0.10	91.90±2.69	91.83	143.40±1.099
6	white crystalline powder	10.58±0.31	91.61±2.33	90.78	141.78±1.898
40±2ºC/ 75±5% RH					
0	white crystalline powder	108.92±0.27	91.61±1.76	90.77	144.41±0.317
3	white crystalline powder	110.39±0.24	91.32±2.21	91.40	143.47±0.871
6	white crystalline powder	110.63±0.21	91.90±1.83	90.98	142.98±0.915

a *Observed values: Mean ±S.D., n=3)*

Particle size analysis:

The particle size analysis profile of the optimized freeze dried RM-NSGs (F4) formulation is depicted in Fig 6.76. It was observed that, formulation (F4) showed analogous to that of initial particle size profile which was done before stability. Thus, no significant difference has been revealed in the formulation when exposed even at different temperature and humidity conditions like 25ºC ± 2ºC and RH 60% ± 5%, 30ºC ± 2ºC and RH 65% ± 5% and 40ºC ± 2ºC and RH 75% ± 5% as per the stability guidelines. The particle size study indicated that there was no significant difference observed as compared to the initial particle size profile of optimized freeze dried RM- NSGs.

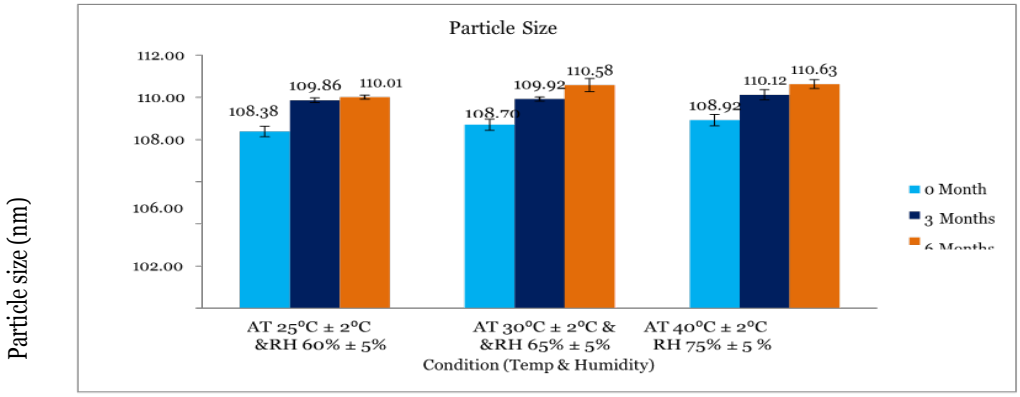

Figure 15: Particle size data of optimized freeze dried RM-NSGs at differenttemperature and humidity conditions

% Entrapment efficiency:

The % entrapment efficiency profile of the optimized freeze dried RM-NSGs (F4) formulation is depicted in Fig 6.77. It was observed that, formulation (F4) showed analogous to that of initial % entrapment efficiency profile which was done before

stability. Thus, no significant difference has been revealed in the formulation when exposed even at different temperature and humidity conditions like 25ºC ± 2ºC and RH 60% ± 5%, 30ºC ± 2ºC and RH 65% ± 5% and 40ºC ± 2ºC and RH 75% ± 5% as per the stability guidelines. The particle size study indicated that there was no significant difference observed as compared to the initial % entrapment efficiency profile of optimized freeze dried RM-NSGs.

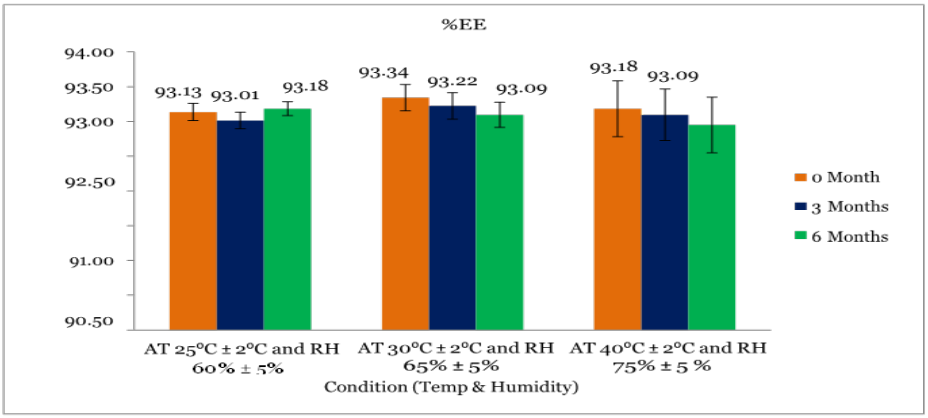

Figure 16: % Entrapment efficiency data of optimized freeze dried RM-NSGs atdifferent temperature and humidity conditions

Summary and conclusion

Factorial design was used for the formulation, development, and assessment of Rasagiline mesylate loaded nanosponges (RM-NSGs), and there in vivo investigation. Idiopathic Parkinson's disease may be treated with rasagiline mesylate, a selective and irreversible monoamine oxidase (MAO)-B inhibitor. A chemically diverse class of medications with the general capacity to inhibit the oxidative deamination of endogenous monoamines. Moreover, this substance belongs to BCS Class III, meaning that its molecules are hydrophilic (high aqueous solubility; water solubility: 0.0249 mg/mL) yet have poor permeability across biological membranes. In under 1 hour, RM reaches its maximum plasma concentration (Cmax). Around 36% of RM gets absorbed into the body. While this chemical has promising pharmacological activity, inadequate bioavailability is achieved owing to poor absorption caused by limited permeability. The permeability characteristics of such a compound have been improved in a number of ways. The techniques range from the more conventional (prodrugs, permeation enhancers, ion-pairing, etc.) to the more cutting-edge (nanoencapsulation, nanosizing, etc.). Our studies support the aforementioned idea by investigating an original strategy for the production of RM-loaded nanosponges' formulation. No prior reports or discussions of a nanosponge RM formulation were found in our research.

Acknowledgement

The authors are thankful to Sunrise University Campus, Bagar Rajput, Alwar, Rajasthan for making available facilities to carry out this work.

Conflicts of interest

The authors declare no conflicts of interests.

Reference

1. Abdelwahed, W. et al., (2006). Freeze-drying of nanoparticles: formulation,

process and storage considerations. Advanced Drug Delivery Reviews 58:1688– 1713.
2. Aderem A (2002). How to eat something bigger than your head. Cell 110:5–8
3. Aderem A, Underhill D (1999). Mechanisms of phagocytosis in macrophages.
4. Annu Rev Immunol 17:593–623.
5. Akbarieh M, Besner JG, Galal A, Tawashi R et. al., (1992). Liposomal system for the targeting and controlled release of praziquantel. Drug Dev Ind Pharm 18:303– 317.
6. Anwar M, Warsi MH, Mallick N et. al., (2011). Enhanced bioavailability of nano- sized chitosan–atorvastatin conjugate after oral administration to rats. Eur J Pharm Sci 44: 241-249.
7. Allen TM, Austin GA, Chonn A, Lin L, Lee KC (1991). Uptake of liposomes by cultured mouse bone marrow macrophages: influence of liposome composition and size. Biochim Biophys Acta Biomembranes 1061:56–64.
8. Anderson JM, Shive MS (1997). Biodegradation and biocompatibility of PLA and PLGA microspheres. Adv Drug Deliv Rev 28:5–24.
9. Arkas M, Allabashi R, Tsiourvas D, Mattausch E, Perfle R (2006). Organic/inorganic hybrid filters based on dendritic and cyclodextrin nanosponges for the removal of organic pollutants from water. Environ Sci Technol 40: 2771- 2777.
10. Amber V, Shailendra S, Swarnalatha S (2008). Cyclodextrin based novel drug delivery systems. J Incl Phenom Macrocycl Chem 62: 23-42.
11. Ahmed R, Patil G, Zaheer Z (2013). Nanosponges–a completely new nano-horizon: pharmaceutical applications and recent advances. Drug Dev Ind Pharm 39: 1263-72.
12. Ansari K, Torne S, Vavia P, Trotta F, Cavalli R (2011). Cyclodextrin -Based Nanosponges for Delivery of Resveratrol: In Vitro Characterization, Stability, Cytotoxicity and Permeation Study. AAPS Pharm Sci Tech 12: 279-86.
13. Amsden B, Misra G, Gu F, Younes H (2004). Synthesis and characterization of a photo-cross-linked biodegradable elastomer. Biomacromolecules 5: 2479-2486.
14. Ali R, Thirumaleshwar S, Bhosale R, Kulkarni P (2014). Nanosponges- The spanking Accession in Drug Delivery-An Updated Comprehensive Review. Der Pharmacia Sinica 5: 7-21.
15. Amidon G, Lennern¨as H, Shah V, and Crison J (1995). A theoretical basis for a biopharmaceutical drug classification: the correlation of in vitro drug product dissolution and in vivo bioavailability. Pharmaceutical Research 12: 413–420,
16. Aulton M (2002). "Dissolution and solubility," in Pharmaceutics: The Science of Dosage form Design, M. E. Aulton, Ed., p. 15,Churchill Livingstone, 2nd edition.
17. Bagade O et. Al., (2020). A Corollary of Nanoporous Carrier Drug Delivery System: An Updated Perspective. International Journal of Pharmaceutical Sciences and Nanotechnology 5: 5047-5061.
18. Bagade O et. Al., (2020). An Influence of Lyophilization on Praziquantel Loaded Nanosponge's by using food protein as a stabilizer with effect of Statistical Optimization. Research J. Pharm. and Tech. 13(9): 4491-4498.
19. Burgess P, Hutt P, Farokhzad O, Langer R et al., (2010). On firm ground: IP protection of therapeutic

nanoparticles. Nat Biotechnol 28: 1267-1270.
20. British Pharmacopoeia, 2009.
21. Brown A, Sheares V (2007). Amorphous unsaturated aliphatic polyesters derived from dicarboxylic monomers synthesized by Diels-Alder chemistry. Macromolecules 40: 4848-4853.
22. Bolmal U, Manvi F, Kotha R, Palla S, Paladugu A, Reddy K (2013). Review on Recent Advances in Nanosponge as Drug Delivery System. Int J PharmSci Nanotech 6: 1934-1944.
23. Black C, Gregoriadis G (1974). Intracellular fate and effect of liposome-entrapped actinomycin-d injected into rats. Biochem Soc Trans 2:869–871.
24. Beningo KA, Wang Y (2002). Fc-receptor-mediated phagocytosis is regulated by mechanical properties of the target. J Cell Sci 115:849–856.
25. Bittencourt P, Gracia C, Gorz A et. al., (1990). High-dose praziquantel for neurocysticercosis: serum and CSF concentrations. Acta Neurologica Scandinavica 82: 28–33.
26. Bareford LM, Swaan PW (2007). Endocytic mechanisms for targeted drug delivery. Adv Drug Deliv Rev 59:748–758.
27. Bagade O (2018). A textbook of Pharmaceutical Quality Assurance, 1st ed. Career Publication, Nashik- India, pp 336.
28. Beckett A, Stenlake J (1997). Practical Pharmaceutical Chemistry, 4th ed, Part II, CBS Publications and Distributors, New Delhi, pp 275-300.
29. Baka E et. al., (2008). Study of equilibrium solubility measurement by saturation shake-flask method using hydrochlorothiazide as model compound. Journal of Pharmaceutical and Biomedical Analysis 46: 335–341.
30. Clugston M and Fleming R (2000). Advanced Chemistry, Oxford Publishing, Oxford, UK, 1st edition.
31. Champion J, Katare K, Mitragotri S (2007). Particle shape: A new design parameter for micro- and nanoscale drug delivery carriers. Journal of Controlled Release 121: 3-9.
32. Chan J, Zhang L, Yuet K, Liao G, Rhee J et al., (2009). PLGA-lecithin-PEG core-shell nanoparticles for controlled drug delivery. Biomaterials 30: 1627-1634.